Research Article
Molecular and Cell Biology

JOURNAL
OF HEPATOLOGY

Integrin β_1-enriched extracellular vesicles mediate monocyte adhesion and promote liver inflammation in murine NASH

Graphical abstract

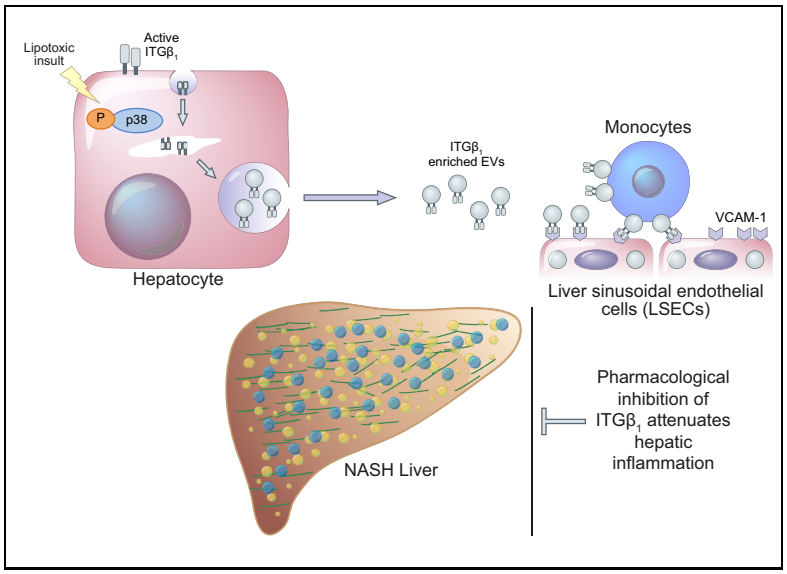

Highlights

- Hepatocytes under lipotoxic stress release active ITGβ_1-enriched EVs.
- Lipotoxic hepatocyte-derived EVs enhance monocyte adhesion to liver sinusoidal endothelial cells mainly via their ITGβ_1 cargo.
- ITGβ_1 neutralizing antibody reduces proinflammatory monocyte hepatic infiltration in murine NASH.
- Blocking ITGβ_1 attenuates liver inflammation, injury and fibrosis in murine NASH.

Authors

Qianqian Guo, Kunimaro Furuta, Fabrice Lucien, ..., Yandong Gao, Alexander Revzin, Samar H. Ibrahim

Correspondence

ibrahim.samar@mayo.edu
(S.H. Ibrahim)

Lay summary

Herein, we report that a cell adhesion molecule termed integrin β_1 (ITGβ_1) plays a key role in the progression of non-alcoholic steatohepatitis (NASH). ITGβ_1 is released from hepatocytes under lipotoxic stress as a cargo of extracellular vesicles, and mediates monocyte adhesion to liver sinusoidal endothelial cells, which is an essential step in hepatic inflammation. In a mouse model of NASH, blocking ITGβ_1 reduces liver inflammation, injury and fibrosis. Hence, ITGβ_1 inhibition may serve as a new therapeutic strategy for NASH.

http://dx.doi.org/10.1016/j.jhep.2019.07.019
 J. Hepatol. 2019, 71, 1193–1205

Research Article
Molecular and Cell Biology

JOURNAL OF HEPATOLOGY

Integrin β_1-enriched extracellular vesicles mediate monocyte adhesion and promote liver inflammation in murine NASH

Qianqian Guo[1,†], Kunimaro Furuta[1,†], Fabrice Lucien[2], Luz Helena Gutierrez Sanchez[3], Petra Hirsova[1], Anuradha Krishnan[1], Ayano Kabashima[1], Kevin D. Pavelko[4], Benjamin Madden[5], Husam Alhuwaish[6], Yandong Gao[7], Alexander Revzin[7], Samar H. Ibrahim[1,3,*]

[1]*Division of Gastroenterology & Hepatology, Mayo Clinic, Rochester, Minnesota, United States;* [2]*Department of Urology, Mayo Clinic, Rochester, Minnesota, United States;* [3]*Division of Pediatric Gastroenterology, Mayo Clinic, Rochester, Minnesota, United States;* [4]*Department of Immunology, Mayo Clinic, Rochester, Minnesota, United States;* [5]*Proteomics Core Medical Genome Facility, Mayo Clinic, Rochester, Minnesota, United States;* [6]*School of Medicine, The Royal College of Surgeons in Ireland, Ireland;* [7]*Department of Physiology and Biomedical Engineering, Mayo Clinic, Rochester, Minnesota, United States*

Background & Aims: Hepatic recruitment of monocyte-derived macrophages (MoMFs) contributes to the inflammatory response in non-alcoholic steatohepatitis (NASH). However, how hepatocyte lipotoxicity promotes MoMF inflammation is unclear. Here we demonstrate that lipotoxic hepatocyte-derived extracellular vesicles (LPC-EVs) are enriched with active integrin β_1 (ITGβ_1), which promotes monocyte adhesion and liver inflammation in murine NASH.

Methods: Hepatocytes were treated with either vehicle or the toxic lipid mediator lysophosphatidylcholine (LPC); EVs were isolated from the conditioned media and subjected to proteomic analysis. C57BL/6J mice were fed a diet rich in fat, fructose, and cholesterol (FFC) to induce NASH. Mice were treated with anti-ITGβ_1 neutralizing antibody (ITGβ_1Ab) or control IgG isotype.

Results: Ingenuity® Pathway Analysis of the LPC-EV proteome indicated that ITG signaling is an overrepresented canonical pathway. Immunogold electron microscopy and nanoscale flow cytometry confirmed that LPC-EVs were enriched with activated ITGβ_1. Furthermore, we showed that LPC treatment in hepatocytes activates ITGβ_1 and mediates its endocytic trafficking and sorting into EVs. LPC-EVs enhanced monocyte adhesion to liver sinusoidal cells, as observed by shear stress adhesion assay. This adhesion was attenuated in the presence of ITGβ_1Ab. FFC-fed, ITGβ_1Ab-treated mice displayed reduced inflammation, defined by decreased hepatic infiltration and activation of proinflammatory MoMFs, as assessed by immunohistochemistry, mRNA expression, and flow cytometry. Likewise, mass cytometry by time-of-flight on intrahepatic leukocytes showed that ITGβ_1Ab reduced levels of infiltrating proinflammatory monocytes. Furthermore, ITGβ_1Ab treatment significantly ameliorated liver injury and fibrosis.

Conclusions: Lipotoxic EVs mediate monocyte adhesion to LSECs mainly through an ITGβ_1-dependent mechanism. ITGβ_1Ab ameliorates diet-induced NASH in mice by reducing MoMF-driven inflammation, suggesting that blocking ITGβ_1 is a potential anti-inflammatory therapeutic strategy in human NASH.

Lay summary: Herein, we report that a cell adhesion molecule termed integrin β_1 (ITGβ_1) plays a key role in the progression of non-alcoholic steatohepatitis (NASH). ITGβ_1 is released from hepatocytes under lipotoxic stress as a cargo of extracellular vesicles, and mediates monocyte adhesion to liver sinusoidal endothelial cells, which is an essential step in hepatic inflammation. In a mouse model of NASH, blocking ITGβ_1 reduces liver inflammation, injury and fibrosis. Hence, ITGβ_1 inhibition may serve as a new therapeutic strategy for NASH.

Introduction

With the worldwide increase in obesity, non-alcoholic fatty liver disease (NAFLD) is currently the most common chronic liver disease.[1] A subset of patients with NAFLD develop a more severe inflammatory form termed non-alcoholic steatohepatitis (NASH) which can progress to end-stage liver disease. NASH is currently the leading cause of liver-related mortality in many western countries.[2] Therefore, there is an unmet need for mechanism-based therapeutic strategies that reverse established NASH and control the progression of the disease.

Current concepts suggest that excess circulating free fatty acids mediate hepatocyte lipotoxicity in NASH.[3] Moreover, patients with NASH are at risk of end-stage liver disease, mainly secondary to the unrelenting sterile inflammatory response triggered by hepatocyte lipotoxicity. This inflammatory response is mediated, in part, by the recruited monocytes that differentiate into macrophages, so-called monocyte-derived macrophages (MoMFs).[4] Although targeting monocyte infiltration in NASH via the dual CC chemokine receptor types 2 and 5 (CCR2/5) antagonist improved fibrosis, it was insufficient to resolve human steatohepatitis.[5] Therefore, key additional signals regulating the trafficking and retention of circulating monocytes in the NASH liver remain undefined.

Keywords: Extracellular vesicles; Integrin β_1; Integrin α_9; Adhesion; Inflammation; NASH; Monocytes; Liver sinusoidal endothelial cells; Mass cytometry; Fibrosis.
Received 17 April 2019; received in revised form 8 July 2019; accepted 15 July 2019; available online 6 August 2019

* Corresponding author. Address: Division of Pediatric Gastroenterology, Department of Pediatric and Adolescent Medicine, Mayo Clinic, 200 First Street SW, Rochester, MN 55905, United States. Tel.: +1 (507) 266 0114; fax: +1 (507) 284 0160.
E-mail address: ibrahim.samar@mayo.edu (S.H. Ibrahim).
† These authors contributed equally to the manuscript.

Hepatocytes release diverse types of membrane-bound, nanometer-sized extracellular vesicles (EVs) into the extracellular milieu under physiological conditions. EVs are efficient messengers, with superior stability and bioavailability of their signature cargos implicated in inflammatory responses.[6–8] Interestingly, many of the EV cargos are selectively transferred through intracellular trafficking pathways and packaged into EVs, reflecting the pathophysiological context of the parent cell.[9] EVs released from lipotoxic hepatocytes are involved in MoMF chemotaxis and the hepatic inflammatory response,[6–8] however, the role of lipotoxic hepatocyte-derived EVs (lipotoxic EVs) in promoting circulating monocyte liver-specific homing through regulating their adhesion to liver sinusoidal endothelial cells (LSECs) in the NASH liver microenvironment has not been explored.

LSECs are highly specialized endothelial cells that serve as a platform for various immune cells, including monocytes, to lodge in the liver.[10] As monocyte receptor-LSEC ligand interactions are not unique to the liver, the question remains whether hepatocyte-specific recruitment processes via EVs exists in NASH. A single prior study reported that adoptive transfer of EVs isolated from the serum of high fat diet-fed mice into chow-fed mice resulted in myeloid cell activation and accumulation in the liver.[11] However, the mechanism by which EVs mediate the hepatic accumulation of myeloid cells was not explored.

Integrins (ITGs) provide the central mechanism for cells in multicellular organisms to interact with and sense their extracellular environment.[12] Integrins are heterodimeric cell surface transmembrane proteins consisting of 24 non-covalently associated α and β subunits which mediate cell-cell and cell-matrix interaction.[13] ITGα_9 and β_1 exist as heterodimers, and our data indicate that they are particularly enriched in EVs derived from lipotoxic hepatocytes; hence we will use ITGβ_1 for simplicity in this manuscript to refer to ITG$\alpha_9\beta_1$. Vascular cell adhesion molecule 1 (VCAM-1) is expressed on the surface of LSECs and is a known ligand for ITG$\alpha_9\beta_1$.[14] Interestingly, ITG can adopt a closed conformation that has a low affinity for ligand (inactive) or an extended open conformation that has a high affinity for ligand (active).[15] Binding of intracellular proteins such as Talin to the dephosphorylated cytoplasmic tail of ITGβ_1 regulates its activation and promotes ligand binding.[15] Kinase p38 has been implicated in ITGβ activation *via* an inside-out, ligand-independent signaling in different disease models.[16,17] We have previously demonstrated that lipotoxic treatment in hepatocytes induces a mitogen-activated protein kinase (MAPK) signaling cascade leading to the activated phosphorylation of p38.[6,18,19] Moreover, ITGs undergo constant endocytic trafficking and recycling that regulate ITG-mediated cell adhesion and migration.[20,21] This process of ITG trafficking suggests that in lipotoxic hepatocytes, ITGβ_1 traffics through the endocytic-multivesicular body (MVB) pathway to be released in EVs.

Herein we report that ITGβ_1, a highly expressed ITG in hepatocytes,[22] is enriched and in an active status in lipotoxic EVs. ITGβ_1-enriched EVs enhance monocyte adhesion to LSECs. Most importantly, we demonstrate that ITGβ_1 neutralizing antibody attenuates diet-induced NASH in mice, mainly by reducing proinflammatory monocyte hepatic infiltration.

Materials and methods

Nanoscale flow cytometry

EVs derived from cell culture medium or human serum were labelled with the active conformation sensitive ITGβ1 antibody 9EG7 and analyzed using the A50-Micro Plus nanoscale flow cytometry (Apogee FlowSystems Inc.).

Adhesion assay

A flow-based shear stress adhesion assay consisting of a microfluidic chamber, syringe pump and inverted phase microscope was employed to assess adhesion of monocytes to LSECs. Liver sinusoidal endothelial cells were seeded in the chamber channel. Monocytes were incubated overnight with EVs, infused through the chamber at a constant shear stress of 0.01 Pa for 5 min. Adherent monocytes were imaged and quantified using ImageJ software.

Animals

Study protocols were conducted as approved by the Institutional Animal Care and Use Committee (IACUC) of Mayo Clinic. C57BL/6J male mice were purchased from Jackson Laboratory. Eight-week-old mice were fed either a chow diet or a diet rich in fat, fructose, and cholesterol (FFC) (AIN-76A Western Diet, TestDiet, St Louis, MO) for 24 weeks. At 20 weeks on the diet, mice were randomized to receive either anti-ITGβ1 neutralization antibody (Hmb1-1) or IgG isotype antibody at a dose of 1 μg/g body weight intraperitoneally, twice per week for 4 weeks. Intrahepatic mouse leukocytes were isolated using liver dissociation kit and Percoll gradient centrifugation and subjected to flow cytometry and mass cytometry by time-of-flight (CyTOF) analysis.

Full details of the materials and methods are included in the supplementary information.

Results

Lipotoxic hepatocyte-derived EVs are enriched with integrins

We adopted a non-biased approach to identify and characterize the key proteins on lipotoxic hepatocyte-derived EVs. To this end, we performed proteomics analysis by mass spectrometry (MS) on the EVs derived from primary mouse hepatocytes (PMHs) treated with vehicle (Veh) and the toxic lipid mediator lysophosphatidylcholine (LPC). We employed LPC since the toxicity of the saturated free fatty acid palmitate is dependent upon its metabolism to LPC.[23,24] Unbiased Ingenuity® pathway analysis (IPA) of the proteomics data identified ITG signaling among the top represented canonical pathways, particularly in EVs from LPC-treated hepatocytes when compared to EVs from vehicle-treated hepatocytes (Fig. 1A). Next, we performed immunoblot analysis for different ITGs in hepatocytes treated with vehicle and LPC, and their derived EVs. Western blot identified selective enrichment of ITGβ_1, ITGα_5, ITGα_9, and ITGα_v in EVs released from lipotoxic PMH, without changes at the cellular levels (Fig. 1B). Similar results were obtained with the human hepatoma cell line Huh7 (Fig. 1C). Since ITGβ_1 is the most abundant ITG on hepatocytes[22] and the only ITGβ expressed on EVs based on our MS data, we focused on ITGβ_1 as the key functional ITG family member on lipotoxic EVs. Interestingly, the protein level of Talin-1 (a versatile ITGβ_1 affinity regulator implicated in adhesion)[25] was also increased in lipotoxic EVs, suggesting that the ITGβ_1 on lipotoxic EVs is in active conformation status. To confirm this observation, we employed immunogold electron microscopy, and demonstrated using the active conformation sensitive ITGβ_1 antibody (9EG7) enrichment of ITGβ_1 in EVs released from lipotoxic PMH (Fig. 1D). This observation was further confirmed by nanoscale

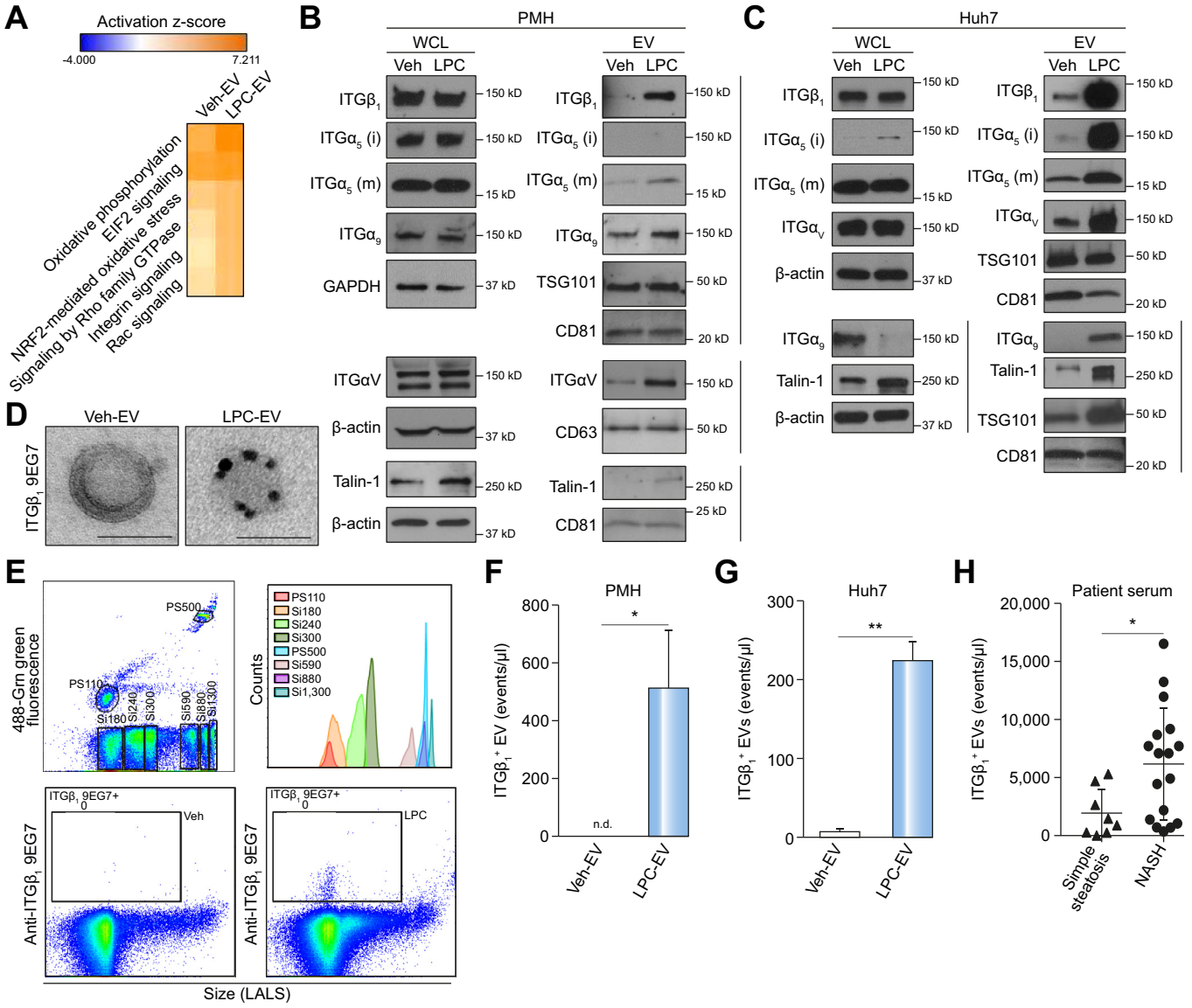

Fig. 1. Lipotoxic hepatocyte-derived EVs are enriched with active ITGβ$_1$. (A) Top ranked canonical pathways identified by IPA of proteomic data on EVs derived from vehicle or LPC-treated PMHs. Immunoblot analysis showing protein levels of integrin family members and Talin-1 on EVs and WCL from (B) PMHs or (C) Huh7 cells treated with vehicle or 20 μM LPC for 4 h. Beta-actin, and the EV markers TSG101, CD63 and CD81 were used as loading controls for WCL and EVs, respectively. (D) Immunogold electron microscopy images showing immunoreactivity for ITGβ$_1$ in an active conformation on EVs derived from PMHs treated with vehicle (Veh-EV) or LPC (LPC-EV). Nanoscale flow cytometry showing expression levels of active ITGβ$_1$ on EVs, (E) various sizes silica nanoparticles used as calibration beads to define EVs based on the particle size (top panel). ITGβ$_1^+$ EVs from PMHs treated with Veh or LPC (bottom panel), quantification of ITGβ$_1$-positive EVs from (F) PMH and (G) Huh7. Bar columns represent mean ± standard error of the mean (SEM); n = 3–5. (H) Quantification of ITGβ$_1^+$ EVs in the serum of patients with simple steatosis (n = 8), and NASH with stage 1–2 fibrosis (n = 17). Graphs represent mean ± SEM; $^*p$ <0.05, $^{**}p$ <0.01 (Unpaired *t* test). EVs, extracellular vesicles; LPC, lysophosphatidylcholine; PMHs, primary mouse hepatocytes; WCL, whole cell lysate.

flow cytometry, which allows the quantification of active ITGβ$_1$-bearing EVs. LPC-treated PMH released more abundant active ITGβ$_1$-positive EVs compared to Veh-treated PMHs (Fig. 1F). These findings were also confirmed using Huh7 cells (Fig. 1G). Interestingly ITGβ$_1$ expression was increased in the serum EVs of patients with NASH (Fig. 1H). Collectively, these data indicate that ITGβ$_1$ in an active conformation is selectively sorted into EVs released from lipotoxic hepatocytes.

Hepatocyte lipotoxic treatment induces ITGβ1 activation and endocytic trafficking

We further examined the activation and endocytic trafficking of ITGβ$_1$ in hepatocytes under lipotoxic stress (Fig. 2A). Conformation-specific antibodies against ITGβ$_1$ cannot detect the SDS-denatured target protein, and thus are not suitable for immunoblot assay. Therefore, to determine if hepatocyte ITGβ$_1$ is activated by lipotoxic treatment, lysates from Veh or LPC-treated Huh7 cells were immunoprecipitated with the inactive (MAB13) or the active (9EG7) conformation-specific ITGβ$_1$ antibodies, and immunoblotted with an antibody for total ITGβ$_1$ (Fig. 2B). Based on our prior report of p38 activation with lipotoxic treatment in hepatocytes,[6,19] and the established role of p38 in ITG activation in different disease models,[16,17] we examined whether p38 mediates LPC-induced ITGβ$_1$ activation in hepatocyte. LPC treatment causes a significant decrease in inactive (tyrosine phosphorylated ITGβ$_1$ tail, higher molecular

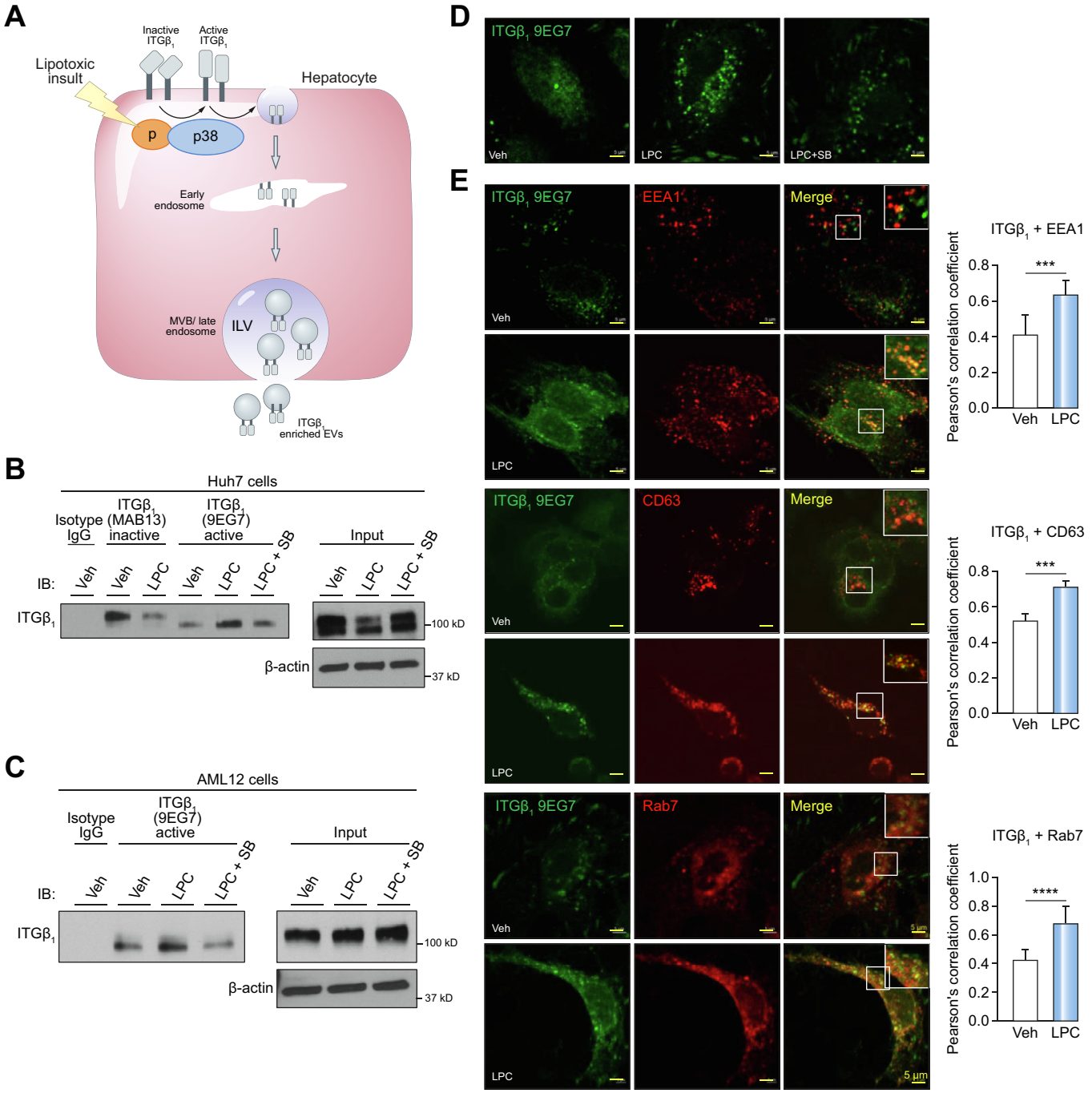

Fig. 2. Hepatocyte lipotoxic treatment induces ITGβ$_1$ activation and endocytic trafficking. (A) Schematic representation of activation and endocytic trafficking of ITGβ$_1$. (B) Huh7 cells and (C) AML12 cells were treated with either vehicle or 20 μM LPC for 15–30 min ± 10 μM p38 inhibitor SB203580 (SB). Cell lysates were immunoprecipitated with active conformation-sensitive ITGβ$_1$ antibody (9EG7), inactive conformation-sensitive ITGβ$_1$ antibody (Mab13) or isotype IgG. Beta-actin was used as a loading control. Huh7 cells were treated with either vehicle or 5 μM LPC for 20 min ± 10 μM SB203580, (D) active ITGβ$_1$ was labeled with 9EG7. (E) Co-localization of active ITGβ$_1$ with early endosomes, late endosomes, or MVBs was assessed using anti-EEA1, anti-Rab7, and anti-CD63 antibodies, respectively. Scale bar: 5 μm, n = 3, quantification of co-localization between 2 fluorophores was done by Pearson's correlation coefficient; ***p <0.001, ****p <0.0001 (Unpaired t test). MVB, multivesicular body.

weight), and increase in active (tyrosine dephosphorylated tail, lower molecular weight) ITGβ$_1$, which is reduced in the presence of the p38 inhibitor SB203580, indicating that lipotoxic stress-induced hepatocyte ITGβ$_1$ activation occurs via a p38-mediated pathway. Similar results were obtained with the mouse hepatocyte cell line AML12 (Fig. 2C), (the inactive conformation sensitive antibody MAB13 reacts only with human species hence it was not used with the mouse AML12 cells). To confirm that the ITGβ$_1$ 9EG7 antibody immunoprecipitates active ITGβ$_1$, we analyzed the ITGβ$_1$ immunoprecipitates from vehicle and LPC-treated PMHs by MS, as previously described by us.[6] The MS data was searched allowing for phosphostyrosine as a variable modification and showed absence of phosphorylation on the first NPxY motif on the ITGβ$_1$ C terminal,

confirming that the pulled ITGβ_1 is in an active conformation (Table S1). Furthermore, we employed immunofluorescence (IF) microscopy and confirmed that LPC treatment induced activation of ITGβ_1, which was diminished with SB203580 (Fig. 2D). Moreover, we noted that in lipotoxic hepatocytes, the active ITGβ_1 accumulated in cytoplasmic structures consistent with intracellular vesicles (Fig. 2D, second panel). To further explore the intracellular trafficking of active ITGβ_1, we examined the co-localization of active ITGβ_1 with the early endosome marker early endosome antigen (EEA) 1, the MVB marker CD63, and the late endosome marker Rab7. ITGβ_1 co-localization with EEA1, CD63 or Rab7 (Fig. 2E) was increased with LPC treatment when quantified using the Pearson's correlation coefficient. To examine if lipotoxicity regulates active ITGβ_1 lysosomal degradation, we assessed the co-localization of active ITGβ_1 with the lysosome marker LAMP1; however, there was no obvious co-localization of ITGβ_1 with LAMP1 (Fig. S1). Collectively, these results suggest that hepatocyte lipotoxic treatment induces ITGβ_1 activation and endocytic trafficking, resulting in active ITGβ_1 release in EVs.

Lipotoxic hepatocytes release EVs in the circulation

We have previously demonstrated that LPC treatment increases hepatocytes EVs release *in vitro*.[6,8] To assure that this observation is not an artifact of the *in vitro* system, we developed a mouse model to track circulating EVs of hepatocyte origin (Fig. S2A). We then quantified the hepatocyte-derived EVs in the plasma by nanoscale flowcyometry, and identified a 5-fold increase with the NASH-inducing diet (Fig. S3B). These data conclusively demonstrate for the first time that lipotoxic hepatocytes release large number of EVs in the circulation *in vivo*.

Lipotoxic hepatocyte-derived EVs promote monocytes adhesion to LSECs via an ITGβ_1-dependent mechanism

We have previously reported that EVs from lipotoxic hepatocytes induce MoMF chemotaxis.[6] To understand the biological functions exerted by lipotoxic hepatocyte-derived EVs on monocytes, we performed RNA sequencing (RNAseq) on primary mouse monocytes incubated with EVs from LPC (LPC-EVs) or vehicle (Veh-EVs)-treated PMHs. IPA of RNAseq data showed leukocyte adhesion and diapedesis-related signaling among the top overrepresented canonical pathways in monocytes stimulated with LPC-EVs, suggesting the involvement of LPC-EVs in monocyte adhesion to LSECs (Fig. 3A).

To examine the interaction between lipotoxic EV-stimulated monocytes and LSECs, we co-cultured the human monocyte cell line, THP1, with EVs derived from equal number of hepatocytes treated with either vehicle or LPC. EVs were labelled with a fluorescent lipophilic dye DiO. Confocal microscopy revealed that monocytes incubated with LPC-EVs were more likely to adhere to LSECs (Fig. 3B). We then subjected monocytes to live cell imaging with Z stack microscopy following incubation with EVs. EVs were observed both on the surface and on deeper focal plane (intracellular) of the THP1 cells (Fig. 3C), suggesting that ITGβ_1-enriched EVs interact with monocytes in a topography that allows them to potentially tether monocytes to LSECs. Interestingly, many of these EVs are also internalized by monocytes (Fig. 3C), which has implications for ITGβ_1 recycling to the cell surface. To further explore if LPC-EVs enriched with ITGβ_1 mediates monocyte adhesion to LSECs, a key stage in liver inflammation, we employed a flow-based adhesion assay using microfluidic chambers (Fig. S3A-B) coated with a monolayer of mouse primary LSECs. Monocytes stimulated with LPC-EVs have enhanced adhesion to LSECs (Fig. 3D). Interestingly this enhanced adhesion was diminished when monocytes were incubated with anti-ITGβ_1 neutralizing antibody (ITGβ_1Ab), suggesting that ITGβ_1 on lipotoxic EVs may be responsible for EVs-induced monocytes adhesion to LSECs. We further confirmed this finding using ITGβ_1-knockdown Huh7 by shRNA technology (shITGβ_1) (Fig. 3E-F, Fig. S3C). Likewise, the adhesion of lipotoxic EV-stimulated monocytes to endothelial cells was reduced in the presence of ITGα_9 neutralizing antibody (Fig. S3D). Moreover, pretreatment of LSECs with a neutralizing antibody against VCAM-1 (an ITG$\alpha_9\beta_1$ ligand expressed on LSECs under basal conditions as examined by flow cytometry), significantly diminished the adhesion of LPC-EV-stimulated monocytes to LSECs (Fig. 3F). Taken together, these results support a role for LPC-EV ITG$\alpha_9\beta_1$ in monocyte adhesion to LSEC via an ITG$\alpha_9\beta_1$-VCAM-1 binding interactions. Interestingly, monocyte inflammatory activation markers expression was also enhanced with lipotoxic EV stimulation (Fig. S4), supporting the proinflammatory role of lipotoxic EVs.

Anti-ITGβ1 antibody treatment does not alter the metabolic phenotype or the steatosis in FFC diet-fed mice

Based on the *in vitro* findings supporting a key role of lipotoxic EV ITGβ_1 in monocyte adhesion to LSECs and potentially in liver inflammation, we examined the potential beneficial effect of ITGβ_1 neutralizing antibody in our mouse model of diet-induced NASH. Eight-week-old C57BL/6J wild-type mice were fed either chow or a diet high in saturated FFC for 24 weeks. At 20 weeks of the diet mice were treated with either anti-ITGβ_1 neutralizing antibody (ITGβ_1Ab) or control IgG isotype antibody (IgG) twice per week for 4 weeks. Firstly, we assessed the metabolic status of each group of mice. Comprehensive Laboratory Animal Monitoring System study showed that total daily caloric intake (Fig. S5A), physical activity, energy expenditure, and respiratory quotient (Fig. 4A) were similar in the FFC-fed ITGβ_1Ab-treated and control IgG-treated mice. Body weight during the whole study period (Fig. 4B, Fig. S5B), liver weight (Fig. S5C), and liver to body weight ratio (Fig. 4C) at the time of sacrifice were significantly increased with the FFC diet, but similar between ITGβ_1Ab-treated and control IgG-treated groups. Likewise, homeostasis model assessment of insulin resistance (HOMA-IR) (Fig. 4D), and triglyceride content in liver tissue (Fig. 4E) were increased with the FFC diet, but were not different between the 2 treatment groups on the FFC diet; although HOMA-IR has some limitations in assessing insulin sensitivity *in vivo*. Moreover, histological examination of the liver by hematoxylin and eosin (H&E) stain displayed similar extent of steatosis in the FFC-fed mice from the different treatment groups (Fig. 4F). Interestingly, ITGβ_1Ab-treated mice had less inflammatory infiltrates compared to IgG-treated, FFC-fed mice (Fig. 4F). Consistent with the *in vitro* data, active ITGβ_1 expression was increased with FFC diet when assessed by immunohistochemistry and reduced with the ITGβ_1 neutralizing Ab (Fig. S6A). Collectively, ITGβ_1Ab treatment in FFC-fed mice was well tolerated and did not affect the metabolic phenotype or the hepatic steatosis.

Anti-ITGβ_1 antibody treatment in FFC-fed mice attenuates hepatic inflammation

Given the key role of ITGβ_1 in monocyte adhesion to LSECs (Fig. 3D-F), we examined whether ITGβ_1Ab reduces hepatic

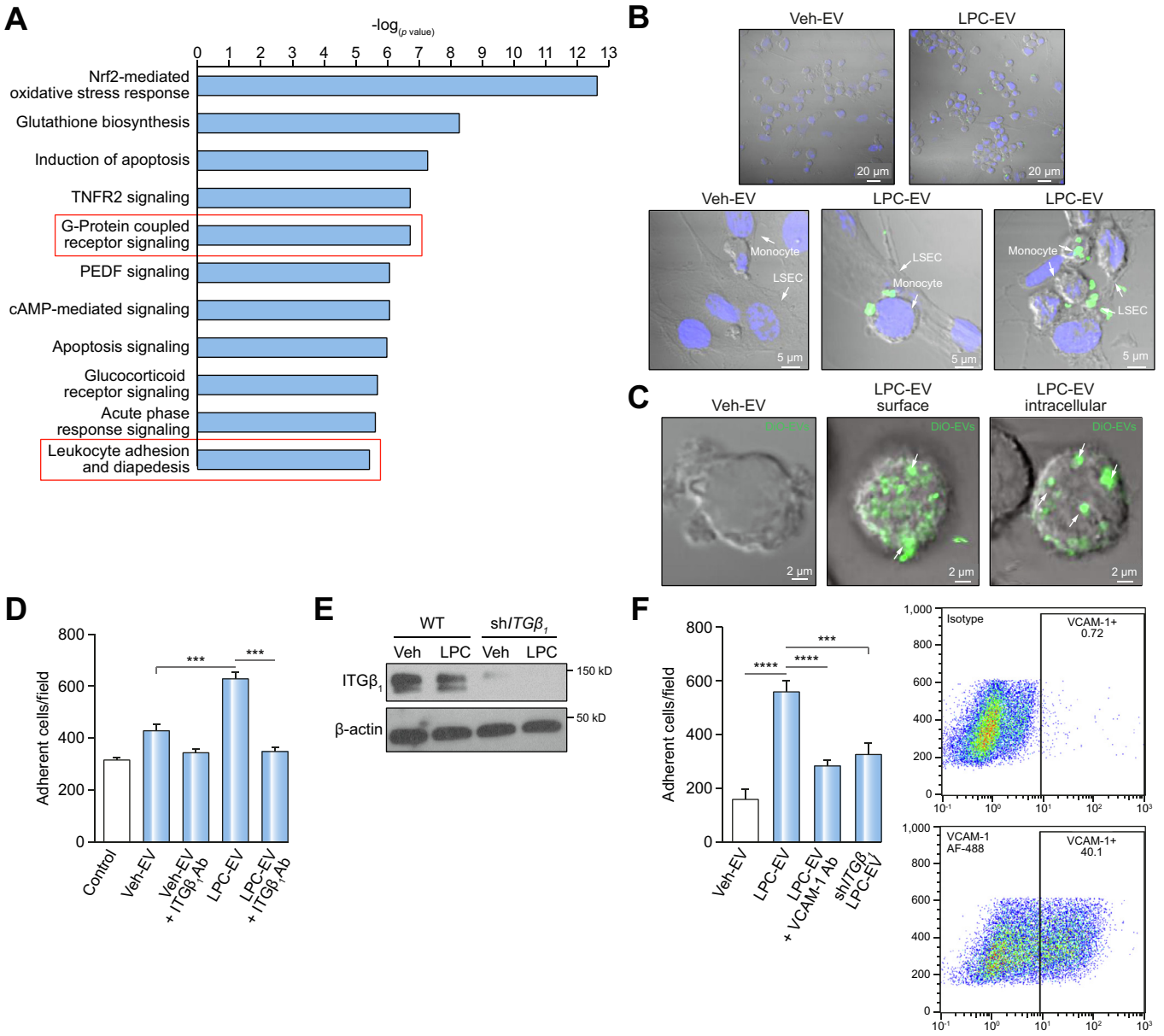

Fig. 3. Lipotoxic hepatocyte-derived EVs promote monocyte adhesion to LSECs via an ITGβ$_1$-dependent mechanism. (A) Top represented canonical pathways in monocytes stimulated with LPC-EVs *vs.* Veh-EVs. (B) Equal number of Huh7 cells were treated with either veh or LPC. EVs were collected from the conditioned media and labelled with DiO. THP1 cells were co-cultured with human LSECs in the presence of labelled EVs. Scale bar: 20 µm for the top panel, and 5 µm for the bottom panel. (C) Z stack confocal microscopy of THP1 incubated with DiO-labelled EVs from LPC-treated Huh7 cells (white arrows). (D) Primary mouse monocytes were stimulated with Veh-EV or LPC-EV from PMH ± ITGβ$_1$Ab, and infused in microfluidic chambers coated with a monolayer of primary mouse LSECs. Adherent cells were quantified. (E) Immunoblot analysis showing ITGβ$_1$ knockdown in shITGβ$_1$ cell line. Beta-actin was used as a loading control. (F) THP1 cells were stimulated with either Veh-EV or LPC-EV from wild-type (WT) Huh7 cells, or shITGβ$_1$ Huh7 cells, and infused in microfluidic chambers coated with a monolayer of primary human LSECs ± VCAM-1 Ab. Adherent THP1 cells were quantified similar to D. VCAM-1 is expressed on human LSECs under basal condition as shown by flow cytometry; bar graphs represent mean ± SEM; n = 6, ***p <0.001, ****p <0.0001 (One-way ANOVA with Bonferroni's multiple comparison). EVs, extracellular vesicles; LPC, lysophosphatidylcholine; LSEC, liver sinusoidal endothelial cells.

proinflammatory monocyte recruitment and macrophage-mediated liver inflammation in our dietary mouse model of NASH. Immunostaining of liver tissues revealed that ITGβ$_1$Ab-treated mice had reduced positive area for Mac-2, a marker of phagocytically active macrophages (Fig. 5A-B). This finding was supported by the decrease in hepatic mRNA expressions of the macrophage marker *Cd68*, the infiltrating proinflammatory monocyte marker *Ccr2*, proinflammatory cytokines *Tnf-α*, *Il12b* (Fig. 5C, Fig. S6B) in FFC-fed ITGβ$_1$Ab-treated mice. Furthermore, flow cytometric analysis of the intrahepatic leukocyte (IHL) population identified an increase in CD45$^+$ cells in the FFC-fed mice, without significant alteration with ITGβ$_1$Ab treatment (Fig. 5D). In contrast, ITGβ$_1$Ab-treated FFC-fed mice did display a significant decrease in the infiltrating proinflammatory monocytes (M1 polarized) defined as CD45$^+$CD11b^{hi}-F4/80^{int}CCR2$^+$ cells. Collectively, these findings suggest that blockade of ITGβ$_1$ reduces hepatic proinflammatory monocyte infiltration and MoMF-mediated liver inflammation.

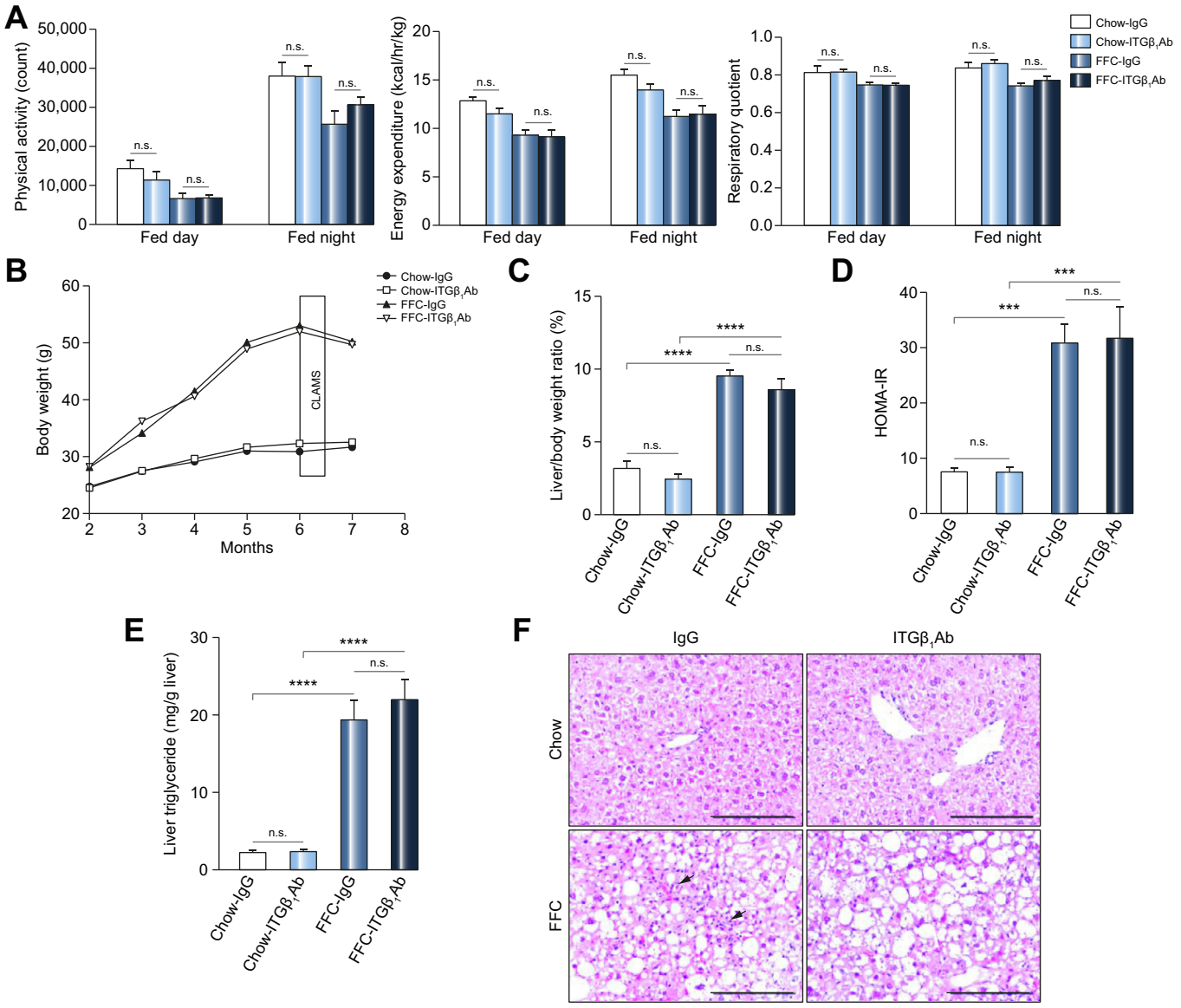

Fig. 4. Anti-ITGβ$_1$ antibody treatment did not alter neither the metabolic phenotype nor the steatosis in FFC diet-fed mice. Wild-type C57BL/6J mice were fed either chow or FFC diet, and treated with either ITGβ$_1$Ab or control IgG isotype. (A) Physical activity, energy expenditure, and respiratory quotient were assessed by Comprehensive Laboratory Animal Monitoring System chambers. (B) Body weight curves. (C) Liver to body weight ratio at the time of sacrifice. (D) HOMA-IR at 23 weeks. (E) Hepatic triglyceride content. (F) Representative images of H&E staining of liver tissues (scale bar, 100 μm). Arrows indicate inflammatory cells infiltrate; bar graphs represent mean ± SEM; ***p <0.001, ****p <0.0001, n.s., nonsignificant; n = 5–6 per group (One-way ANOVA with Bonferroni's multiple comparison). FFC, fat, fructose, and cholesterol; HOMA-IR, homeostasis model assessment of insulin resistance.

Anti-ITGβ$_1$ antibody treatment in FFC-fed mice reduces the proinflammatory monocyte hepatic infiltration

Macrophages are characterized using a variety of criteria, including ontogeny (yolk sac- *vs.* bone marrow-derived) and function (proinflammatory *vs.* restorative).[4] Liver macrophages are also frequently classified as resident macrophages (Kupffer cells) or recruited macrophages (*i.e.*, circulating bone marrow-derived monocytes differentiating into macrophages). Functionally, macrophages exist as a continuum, with tissue damaging or proinflammatory at one end of the spectrum (M1-like), and restorative macrophages involved in tissue repair and healing at the other end (M2-like). While MoMFs play a crucial role in NASH pathogenesis and progression,[26] various other immune cells including neutrophils, dendritic cells, and lymphocytes are involved in NASH pathogenesis.[27,28] Moreover, ITGβ$_1$ neutralizing antibodies are known to inhibit T lymphocyte trafficking,[29] and might also affect neutrophil trafficking to the liver. Therefore, to determine the contribution of the different subset of macrophages, and other immune cells in ITGβ$_1$Ab protective effect in NASH, we profiled B lymphocytes, T lymphocytes, natural killer (NK) cells, NKT cells, dendritic cells and neutrophils in addition to monocytes and macrophages using the state of the art technology mass CyTOF. Twenty-eight clusters were obtained (Fig. 6A) based on the intensities of 24 different cell surface markers (Fig. 6B). Each group of mice displayed a characteristic pattern of clusters abundance (Fig. 6C and D). Out of 28 clusters obtained by CyTOF, 13 clusters were differentially expressed between the study groups and categorized into distinct leukocyte subpopulations based on the intensities of individual cell surface markers (Table S2). In particular, clusters

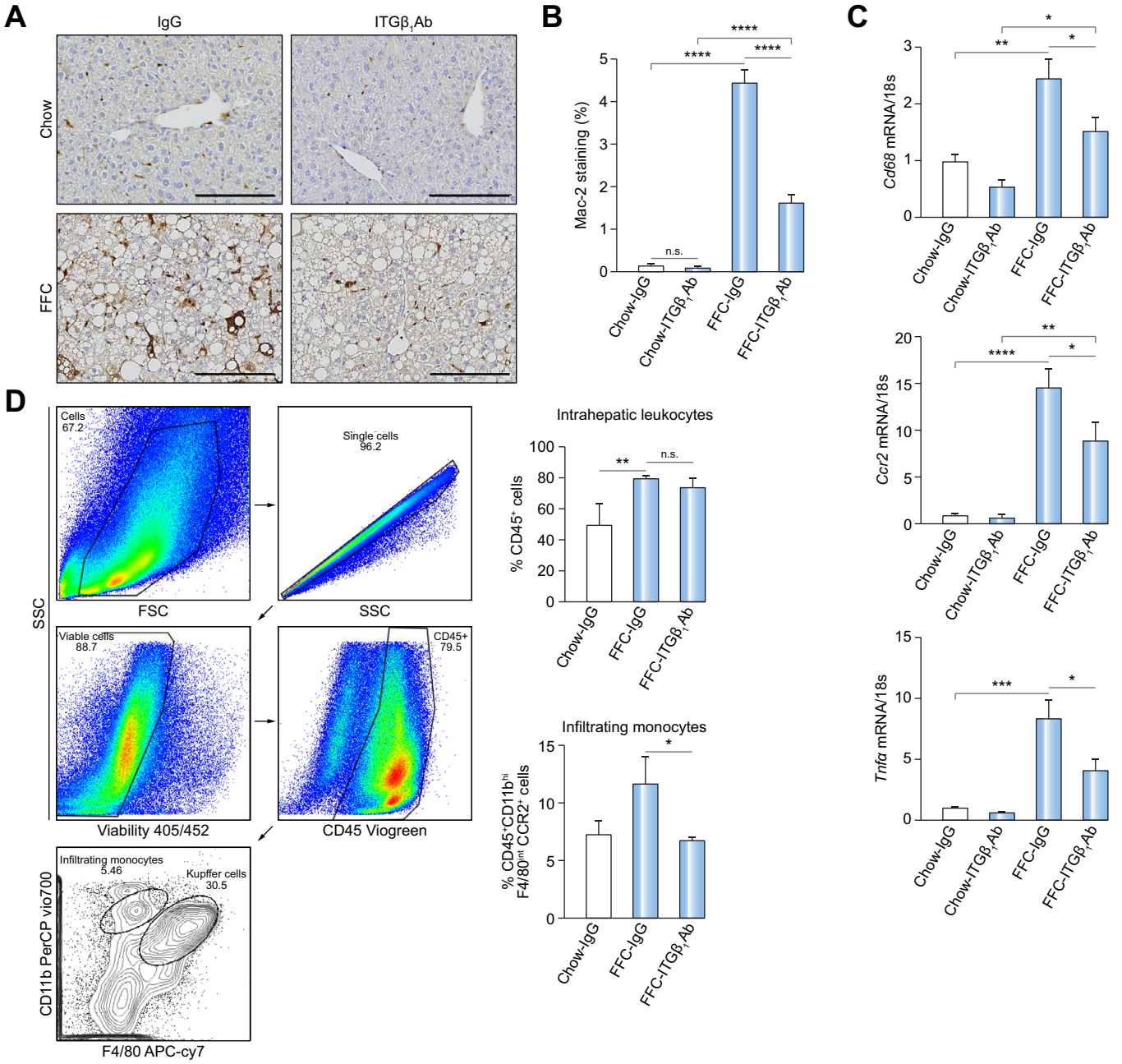

Fig. 5. Anti-ITGβ$_1$ antibody treatment in FFC-fed mice attenuates hepatic inflammation. (A) Representative images of macrophage galactose-specific lectin (Mac-2) staining of liver sections. (B) Mac-2 positive areas were quantified in 10 random 20x microscopic fields and averaged for each animal. (C) Hepatic mRNA expression levels of *Cd68*, *Ccr2* and *Tnf-α* were assessed by real-time PCR. Fold change was determined after normalization to *18 s* expression and expressed relative to Chow-IgG mice. (D) Flow cytometric analysis of the IHL population: top panels show the gating strategy; infiltrating monocytes were defined as CD45$^+$ CD11b^{hi} F4/80^{int} CCR2$^+$cells. Bottom panels show quantification of each population. Bar graphs represent mean ± SEM; n = 3–5 per group; $^*p$ <0.05, $^{**}p$ <0.01, $^{***}p$ <0.001, $^{****}p$ <0.0001 (One-way ANOVA with Bonferroni's multiple comparison, unpaired *t* test for panel D.). FFC, fat, fructose, and cholesterol; IHL, intrahepatic leukocyte.

5 and 9 had typical expression markers of infiltrating proinflammatory MoMFs, the abundance of these clusters was increased with the FFC diet, but significantly reduced with ITGβ$_1$Ab treatment (Fig. 7A), confirming the flow cytometry data. Likewise, clusters 7 and 17 (Fig. 7B) defined as infiltrating MoMFs, were reduced in the FFC-fed ITGβ$_1$Ab-treated mice. In contrast, clusters 1 and 2 had typical marker expression patterns of alternative, M2 polarized, or restorative macrophages defined by increased expression of the anti-inflammatory surface marker CD206, as well as the hepatic macrophage markers Lgals, MERTK, and F4/80. The abundance of clusters 1 and 2 was decreased in the FFC-fed mice, but significantly increased with ITGβ$_1$ blockade (Fig. 7C). We next assessed other clusters defined as B cell-like cluster 8 (Fig. S7A), neutrophil-like cluster 15 (Fig. S7B), dendritic cell-like cluster 19 (Fig. S7C), and T lymphocyte cluster 16 and 21 (Fig. S7D). These clusters showed no statistically significant difference between the FFC-fed experimental groups, indicating that the protective effect of ITGβ$_1$

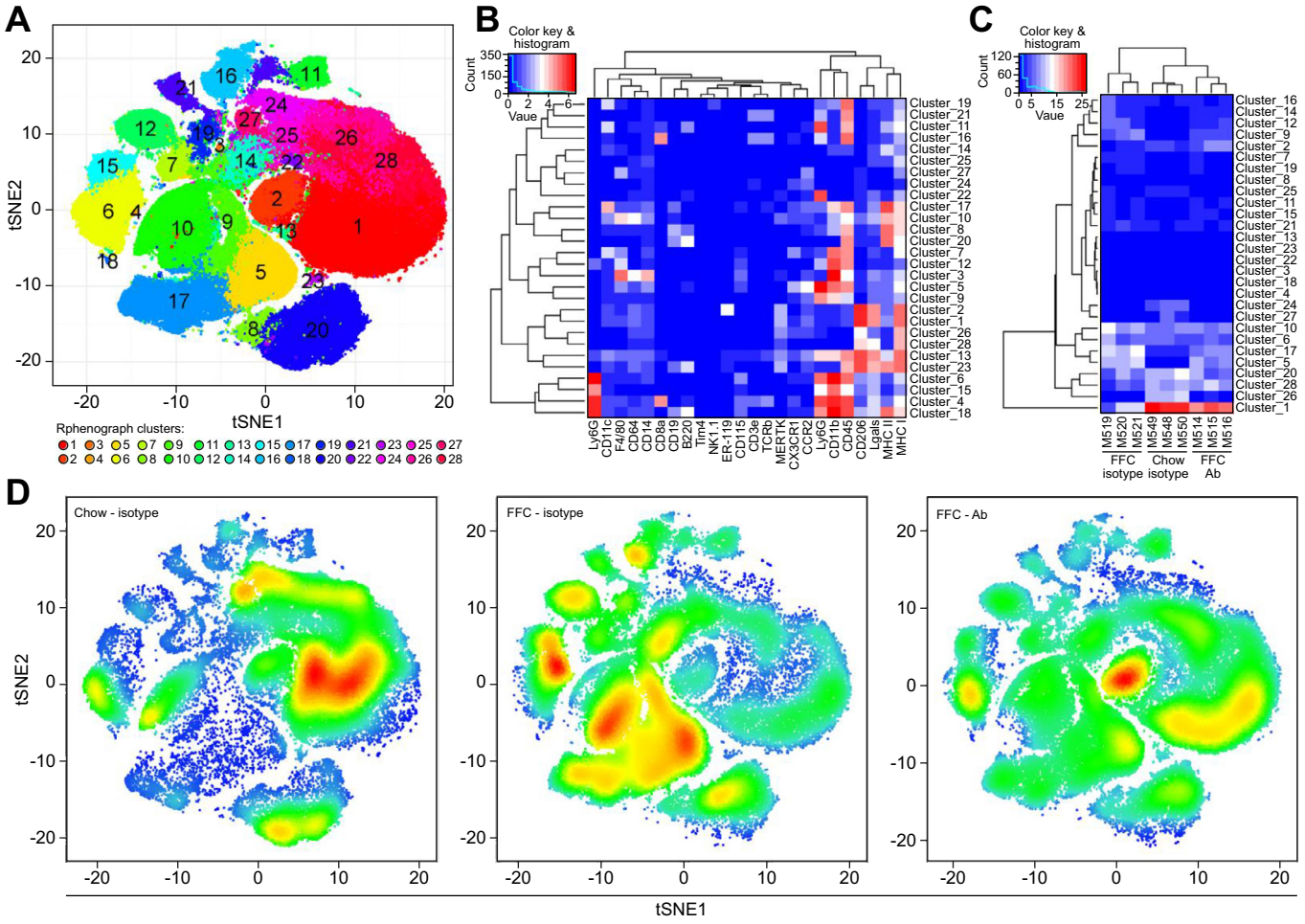

Fig. 6. Intrahepatic leukocyte profiling by mass CyTOF. CyTOF was performed on IHLs of chow-fed mice, and FFC-fed mice treated with either ITGβ_1Ab or control IgG isotype. IHLs from IgG-treated chow-fed mice were used as control. (A) Twenty-eight unique clusters of IHLs were defined by a 24-cell surface marker panel using the Rphenograph clustering algorithm and were visualized on a tSNE plot. (B) Heat map demonstrating the distribution and relative intensity of the cell surface markers used in the clustering analysis. (C) Heat map showing the relative abundance of each cluster for each mouse. (D) Representative tSNE plots of each group. Red indicates high frequency categorization of cells to a cluster; blue indicates low frequency; n = 3 per group. CyTOF, cytometry by time-of-flight; FFC, fat, fructose, and cholesterol; IHL, intrahepatic leukocyte; tSNE, t-distributed stochastic neighbor embedding.

blockade in the FFC diet induced NASH is mainly through reduced proinflammatory monocyte trafficking and retention in the liver without a significant effect on other immune cells.

Anti-ITGβ_1 antibody treatment reduces FFC diet-induced liver injury and fibrosis in murine NASH

To determine if reduced hepatic inflammation through ITGβ_1 blockade may protect against NASH progression and liver fibrosis, we examined liver injury and fibrosis. FFC-fed, ITGβ_1Ab-treated mice were relatively protected against hepatocyte apoptosis compared to control IgG-treated mice, as demonstrated by reduced TUNEL-positive cells (Fig. 8A) and serum alanine aminotransferase levels (Fig. 8B) as well as reduced NAFLD activity score (Fig. 8C) when compared to IgG-treated mice on the same diet. Next, we examined the expressions of fibrosis-related genes, mRNA levels of both Collagen 1a1 *(Col1a1) and* Osteopontin *(Spp1)* were elevated in the FFC-fed mice, and significantly decreased with ITGβ_1Ab treatment (Fig. 8D), indicating the possible anti-fibrotic effect of ITGβ_1Ab. This finding was further confirmed by Sirius red staining (Fig. 8E) as well as α-smooth muscle actin (α-SMA) immunohistochemistry (Fig. 8F). Taken together, these findings indicate a protective effect of ITGβ_1Ab against NASH-associated liver injury and fibrosis in diet-induced NASH.

Discussion

The current study provides insights regarding the mechanism by which lipotoxic hepatocyte-derived EVs may regulate peripheral blood monocyte adhesion to LSECs and hepatic recruitment and retention during NASH. The current data indicate that: i) lipotoxic insult in hepatocyte activates ITGβ_1 and facilitates its endocytic trafficking and release in EVs; ii) lipotoxic hepatocyte-derived EVs enhance monocyte adhesion to LSECs mainly via their ITG$\alpha_9\beta_1$ cargo binding interaction with LSEC VCAM-1; in FFC diet-induced NASH; iii) ITGβ_1 neutralizing antibody reduces proinflammatory monocyte hepatic infiltration; iv) blocking ITGβ_1 attenuates liver injury, inflammation and fibrosis. To our knowledge, our report is the first comprehensive profiling of IHLs in murine NASH using CyTOF, and the first study of a therapeutic effect of ITGβ_1 inhibition in diet-induced NASH. Our findings are discussed in greater details below.

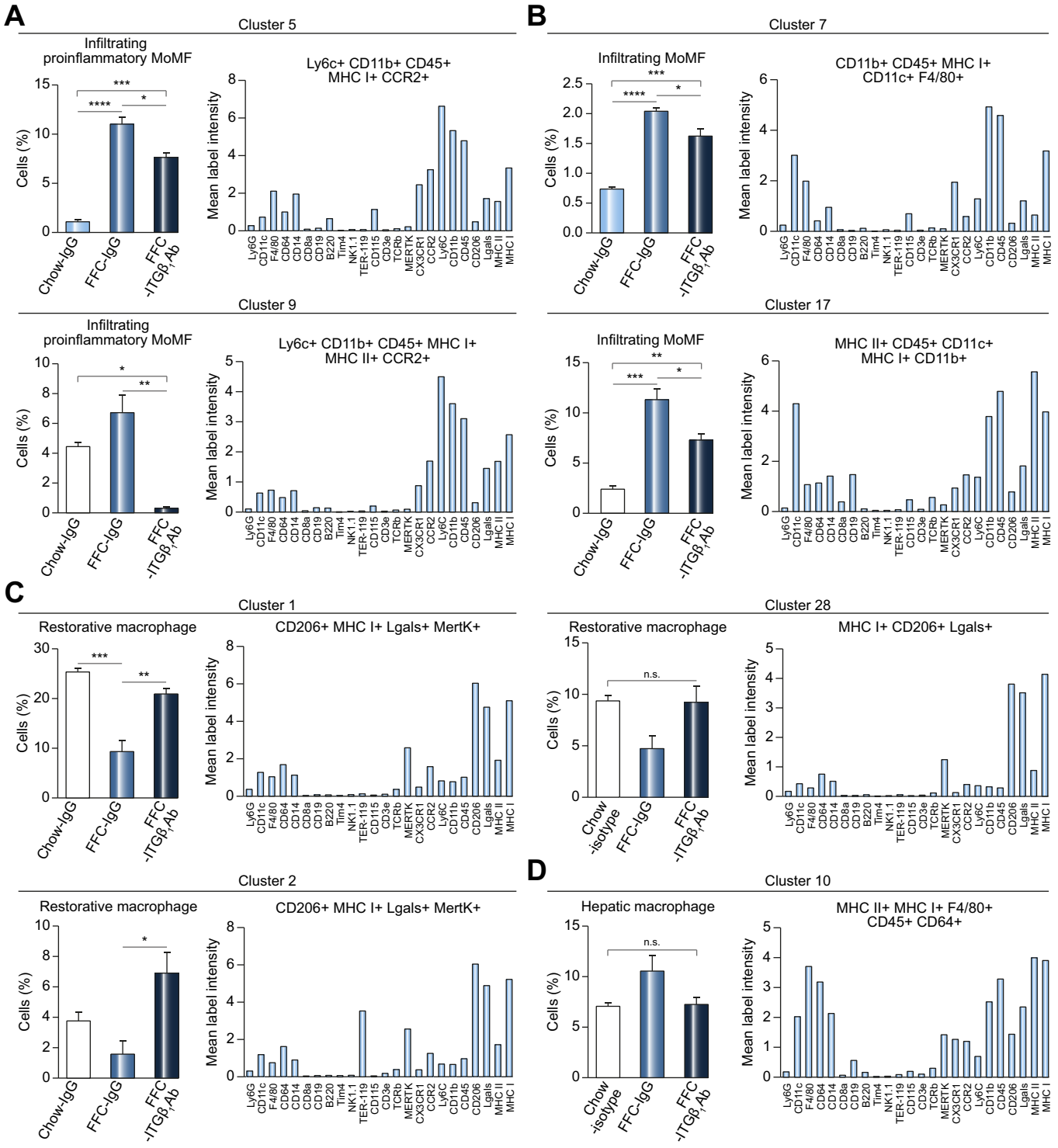

Fig. 7. Anti-ITGβ_1 antibody reduces the proinflammatory monocyte hepatic infiltration in the FFC-fed mice. Differentially expressed clusters between the groups (top graphs); clusters categorized into distinct leukocyte subpopulations based on intensities of individual cell surface markers (bottom graphs). (A) Cluster 5 and 9 represent infiltrating proinflammatory MoMF, (B) clusters 7, and 17 represent infiltrating MoMF, (C) cluster 1, 2 and 28 represent restorative macrophage, and (D) cluster 10 represents hepatic macrophage (n = 3 per group); bar graphs represent mean ± SEM (top panel); *p <0.05, **p <0.01***, p <0.001, ****p <0.0001 (One-way ANOVA with Bonferroni's multiple comparison). FFC, fat, fructose, and cholesterol; MoMFs, monocyte-derived macrophages.

Herein, we build on our prior observation implicating EVs released from lipotoxic hepatocytes in the sterile proinflammatory response in NASH via their chemotactic cargo CXCL10[6] and examine the signaling molecules responsible for monocyte homing to the liver and adhesion to LSECs, a key step for the initiation of inflammation in NASH. We demonstrate for the first time that toxic lipid treatment in hepatocytes induces an active conformation switch of ITGβ_1 via a p38 signaling pathway.

The role of ITG-enriched EVs has been established in organotropism, and tumor cell migration.[21,30] Thus, EV-mediated

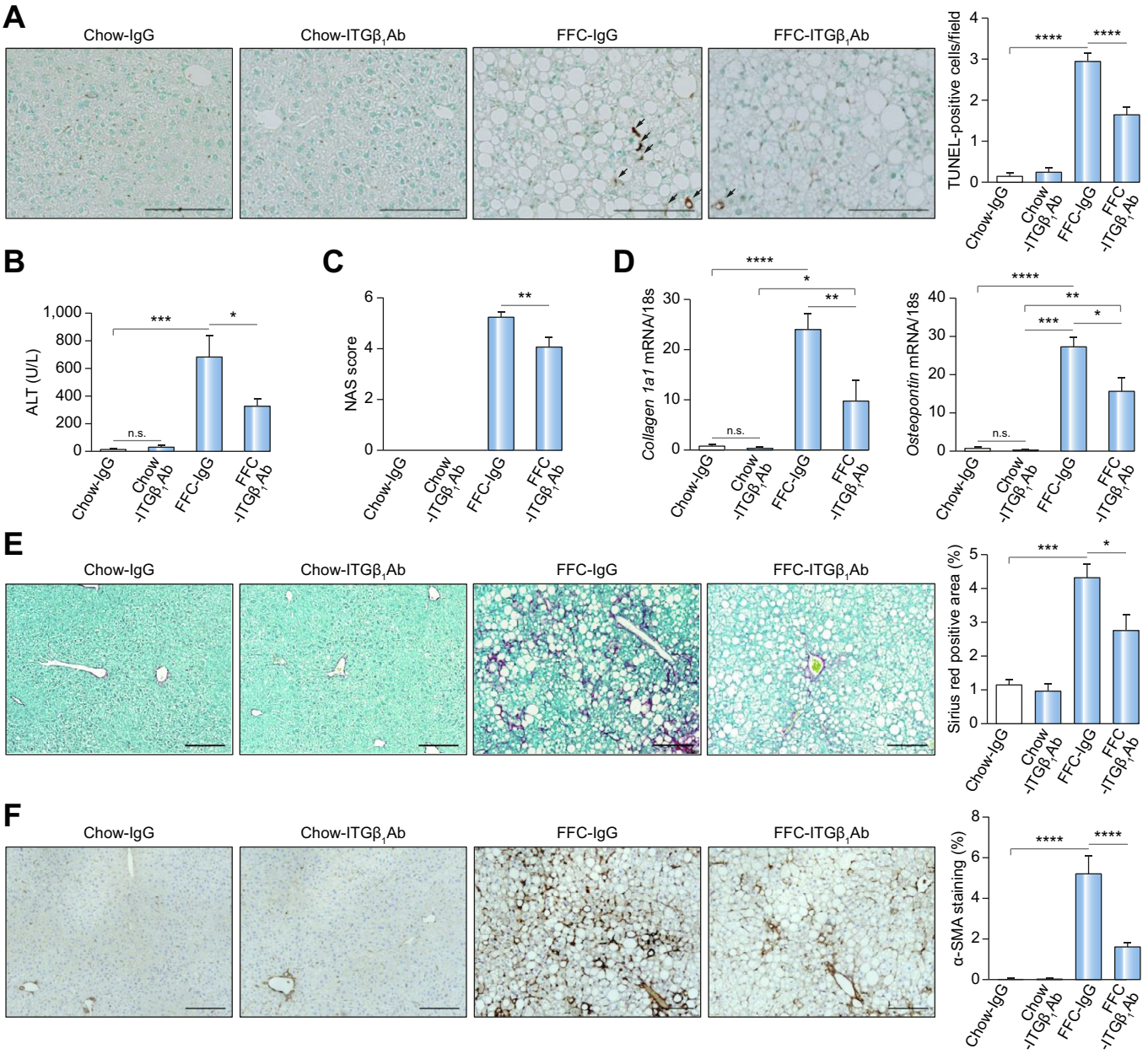

Fig. 8. Anti-ITGβ$_1$ antibody treatment reduces FFC diet-induced liver injury and fibrosis in murine NASH. (A) Representative images of TUNEL staining of liver sections, quantification of TUNEL-positive cells. (B) Serum ALT levels. (C) NAS scores. (D) Hepatic mRNA expression of Collagen1a1 and Osteopontin. (E) Representative images of Sirius red staining, quantification of Sirius red-positive areas. (F) Representative images of α-SMA staining of liver sections, quantification of α-SMA-positive areas. Scale bars: 100 μm; n = 5–6 per group; bar graphs represent mean ± SEM; *p <0.05, **p <0.01, ***p <0.001, ****p <0.0001 (One-way ANOVA with Bonferroni's multiple comparison). ALT, alanine aminotransferase; FFC, fat, fructose, and cholesterol; NAS, NAFLD activity score; NASH, non-alcoholic steatohepatitis.

intercellular ITG signaling is a biologically plausible concept; and our study is the first to identify a non-neoplastic role of ITG on EVs. Moreover, we define the molecular mediators engaged in the adhesion process by employing microfluidic chambers, the optimal technology to study cross talk between 2 different cell types, in a flow-based paradigm[31]. Here we demonstrate that EV-stimulated monocyte adhesion to LSECs was diminished with *Itgβ$_1$* knockdown in the EV donor lipotoxic hepatocytes or with pharmacological inhibition of ITGβ$_1$, ITGα$_9$ or its LSECs ligand VCAM-1. Interestingly, recent *in vivo* study using zebrafish embryo showed targeting of ITGβ$_1$-enriched EVs to the venous endothelium and macrophages.[32] Inspection of tumor-derived EVs in close proximity to the vessel wall revealed arrest of EVs following a rolling behavior, suggesting that it could be driven by progressive activation of adhesion molecules.[32] A very similar behavior was observed for endogenous EVs in zebrafish.[33] Furthermore, EVs either surfed on the filopodia or were taken up by macrophages leading to reduced macrophage motility, and polarization to the M1-like phenotype. Although the exact molecular mediators of the interaction of EVs with both endothelial cells and macrophages were not examined in these studies, these findings relate to ours and support that ITGβ$_1$-enriched EVs interact with monocytes in a topography that enables binding to LSECs, either by fusion/surfing on the cell membrane or endocytosis and recycling back to the surface. Future effort will be concentrated on defining the

molecular mediators responsible for hepatocyte-derived EVs uptake by target cells (LSECs, and MoMFs). Furthermore, our data demonstrate for the first time that the number of circulating EVs of hepatocyte origin is increased in mice with NASH (Fig. S2). The hepatocyte-derived EV gradient is the highest in the liver microenvironment, mainly the sinusoidal space where EVs likely confer the liver homing signal in response to lipotoxic injury. Our findings are also in line with published proteomics analysis of circulating EVs from NAFLD mice, showing enrichment with cell adhesion-related proteins.[34]

To examine the role of ITGβ_1 in monocyte adhesion and liver inflammation *in vivo*, we utilized a well-established dietary mouse model with high fidelity to human NASH.[35] In the current study, we demonstrate that the FFC diet induces similar changes in both ITGβ_1Ab and IgG isotype-treated mice in the metabolic profile and hepatic steatosis. Interestingly, ITGβ_1Ab-treated mice on the FFC diet have a relative attenuation of all the injurious features of NASH, when compared with isotype-treated mice. Moreover, our CyTOF data did not show significant alteration in the T lymphocyte, B lymphocyte, NK cells, neutrophil and dendritic cells populations with ITGβ_1 antibody treatment in FFC-fed mice, suggesting that the therapeutic benefit of ITGβ_1 antibody is mainly through reduced proinflammatory monocyte infiltration.

Inflammation correlates with liver fibrosis and disease progression in NASH patients.[26] Hence, improved liver fibrosis in ITGβ_1Ab-treated FFC-fed mice might be a consequence of reduced MoMF-mediated hepatic inflammation. However, we cannot exclude the possibility that blockade of endogenously expressed ITGβ_1 in other liver cell types such as hepatic stellate cells might have contributed to the reduced fibrosis.

EVs are emerging as key players in cell-to-cell communication. Hence, modulation of EV interaction with target cells by ITGβ_1 pharmacological inhibition would offer a specific therapeutic strategy to block the proinflammatory signal originating from lipotoxic hepatocytes. ITG-based therapeutics have shown clinically significant benefits in patients with chronic inflammatory diseases,[29] and may have an expanded indication for use in patients with NASH. Thus, the current study advances our understanding of the pathogenic mechanisms linking ITG signaling to liver inflammation in NASH, and identify new potential anti-inflammatory therapeutic strategies, that reduces the propensity of LSECs to recruit harmful proinflammatory monocytes.

Financial support

This work was supported by NIH grant DK111397 (to SHI), North American Society of Pediatric Gastroenterology Hepatology and Nutrition Young Investigator Award/Nestle Nutrition Award and Gilead Science career development award (to SHI), the Mayo Clinic K2R pipeline and Children Research Center. F.L is funded by a postdoctoral fellowship from the Fonds de Recherche du Quebec-Sante (FRQS).

Conflict of interest

The authors have no conflict of interest related to the manuscript.

Please refer to the accompanying ICMJE disclosure forms for further details.

Authors' contributions

Q.G.: study design, data acquisition and analysis, manuscript drafting. K.F.: study design, data acquisition and analysis, manuscript drafting. F.L.: data acquisition and analysis, manuscript revision. L.H.G.S: data acquisition. P.H.: data acquisition and manuscript revision. A. Krishnan: data acquisition. A. Kabashima: data acquisition. K.D.P.: data acquisition and analysis, manuscript revision. B.M.: data acquisition and analysis, manuscript revision. H.A.: data acquisition. Y.G.: data acquisition and analysis. A.R.: data acquisition and analysis, manuscript revision. S.H.I.: concept formulation, study design, data analysis, manuscript drafting and revision.

Acknowledgments

We thank Dr. Gregory J. Gores for his thorough review of the manuscript. We thank Dr. Nathan K. LeBrasseur and his laboratory members, especially Dr. Thomas White, for their assistance in the Comprehensive Laboratory Animal Monitoring System data. We thank Dr. Bing Q. Huang for his help in the studies employing electron microscopy. We also thank Dr. Cristine Charlesworth, and the Mayo Clinic Medical Genome Facility-Proteomics Core and its supporting grant, NCI Cancer Center Support Grant 5P30 CA15083-43C1 for performing the mass spectrometry analysis, as well as the optical microscopy core NIDDK P30DK084567.

Supplementary data

Supplementary data to this article can be found online at https://doi.org/10.1016/j.jhep.2019.07.019.

References

Author names in bold designate shared co-first authorship

[1] Bellentani S. The epidemiology of non-alcoholic fatty liver disease. Liver Int 2017;37:81–84.
[2] Younossi ZM. Non-alcoholic fatty liver disease – A global public health perspective. J Hepatol 2019;70:531–544.
[3] Neuschwander-Tetri BA. Hepatic lipotoxicity and the pathogenesis of nonalcoholic steatohepatitis: the central role of nontriglyceride fatty acid metabolites. Hepatology 2010;52:774–788.
[4] Krenkel O, Tacke F. Liver macrophages in tissue homeostasis and disease. Nat Rev Immunol 2017;17:306–321.
[5] **Friedman SL**, **Ratziu V**, Harrison SA, Abdelmalek MF, Aithal GP, Caballeria J, et al. A randomized, placebo-controlled trial of cenicriviroc for treatment of nonalcoholic steatohepatitis with fibrosis. Hepatology 2018;67:1754–1767.
[6] Ibrahim SH, Hirsova P, Tomita K, Bronk SF, Werneburg NW, Harrison SA, et al. Mixed lineage kinase 3 mediates release of C-X-C motif ligand 10-bearing chemotactic extracellular vesicles from lipotoxic hepatocytes. Hepatology 2016;63:731–744.
[7] Hirsova P, Ibrahim SH, Verma VK, Morton LA, Shah VH, LaRusso NF, et al. Extracellular vesicles in liver pathobiology: small particles with big impact. Hepatology 2016;64:2219–2233.
[8] Hirsova P, Ibrahim SH, Krishnan A, Verma VK, Bronk SF, Werneburg NW, et al. Lipid-induced signaling causes release of inflammatory extracellular vesicles from hepatocytes. Gastroenterology 2016;150:956–967.
[9] Anand S, Samuel M, Kumar S, Mathivanan S. Ticket to a bubble ride: Cargo sorting into exosomes and extracellular vesicles. Biochim Biophys Acta Proteins Proteom 2019.
[10] Knolle PA, Wohlleber D. Immunological functions of liver sinusoidal endothelial cells. Cell Mol Immunol 2016;13:347–353.
[11] Deng ZB, Liu YL, Liu CR, Xiang XY, Wang JH, Cheng ZQ, et al. Immature myeloid cells induced by a high-fat diet contribute to liver inflammation. Hepatology 2009;50:1412–1420.
[12] **Massey VL**, **Dolin CE**, Poole LG, Hudson SV, Siow DL, Brock GN, et al. The hepatic "matrisome" responds dynamically to injury: characterization of

transitional changes to the extracellular matrix in mice. Hepatology 2017;65:969–982.
[13] Hynes RO. Integrins: bidirectional, allosteric signaling machines. Cell 2002;110:673–687.
[14] **Humphries JD**, **Byron A**, Humphries MJ. Integrin ligands at a glance. J Cell Sci 2006;119:3901–3903.
[15] Bridgewater RE, Norman JC, Caswell PT. Integrin trafficking at a glance. J Cell Sci 2012;125:3695–3701.
[16] Li Z, Zhang G, Feil R, Han J, Du X. Sequential activation of p38 and ERK pathways by cGMP-dependent protein kinase leading to activation of the platelet integrin alphaIIb beta3. Blood 2006;107:965–972.
[17] **Sun H**, **Liu J**, Zheng Y, Pan Y, Zhang K, Chen J. Distinct chemokine signaling regulates integrin ligand specificity to dictate tissue-specific lymphocyte homing. Dev cell 2014;30:61–70.
[18] Tomita K, Kohli R, MacLaurin BL, Hirsova P, Guo Q, Sanchez LHG, et al. Mixed-lineage kinase 3 pharmacological inhibition attenuates murine nonalcoholic steatohepatitis. JCI Insight 2017:2.
[19] Tomita K, Kabashima A, Freeman BL, Bronk SF, Hirsova P, Ibrahim SH. Mixed lineage kinase 3 mediates the induction of CXCL10 by a STAT1-dependent mechanism during hepatocyte lipotoxicity. J Cell Biochem 2017;118:3249–3259.
[20] Iwamoto DV, Calderwood DA. Regulation of integrin-mediated adhesions. Curr Opin Cell Biol 2015;36:41–47.
[21] Sung BH, Ketova T, Hoshino D, Zijlstra A, Weaver AM. Directional cell movement through tissues is controlled by exosome secretion. Nat Commun 2015:6.
[22] **Bogorad RL**, **Yin H**, Zeigerer A, Nonaka H, Ruda VM, Zerial M, et al. Nanoparticle-formulated siRNA targeting integrins inhibits hepatocellular carcinoma progression in mice. Nat Commun 2014;5:3869.
[23] Kakisaka K, Cazanave SC, Fingas CD, Guicciardi ME, Bronk SF, Werneburg NW, et al. Mechanisms of lysophosphatidylcholine-induced hepatocyte lipoapoptosis. Am J Physiol Gastrointest Liver Physiol 2012;302: G77–G84.
[24] **Piccolis M**, **Bond LM**, Kampmann M, Pulimeno P, Chitraju C, Jayson CBK, et al. Probing the global cellular responses to lipotoxicity caused by saturated fatty acids. Mol Cell 2019;74:32–44 e38.
[25] Tadokoro S, Shattil SJ, Eto K, Tai V, Liddington RC, de Pereda JM, et al. Talin binding to integrin beta tails: a final common step in integrin activation. Science (New York,NY) 2003;302:103–106.
[26] Kazankov K, Jorgensen SMD, Thomsen KL, Moller HJ, Vilstrup H, George J, et al. The role of macrophages in nonalcoholic fatty liver disease and nonalcoholic steatohepatitis. Nat Rev Gastroenterol Hepatol 2019;16:145–159.
[27] Rensen SS, Bieghs V, Xanthoulea S, Arfianti E, Bakker JA, Shiri-Sverdlov R, et al. Neutrophil-derived myeloperoxidase aggravates non-alcoholic steatohepatitis in low-density lipoprotein receptor-deficient mice. PloS ONE 2012;7 e52411.
[28] Li Z, Soloski MJ, Diehl AM. Dietary factors alter hepatic innate immune system in mice with nonalcoholic fatty liver disease. Hepatology 2005;42:880–885.
[29] Ley K, Rivera-Nieves J, Sandborn WJ, Shattil S. Integrin-based therapeutics: biological basis, clinical use and new drugs. Nat Rev Drug Discovery 2016;15:173–183.
[30] **Hoshino A**, **Costa-Silva B**, **Shen TL**, Rodrigues G, Hashimoto A, Tesic Mark M, et al. Tumour exosome integrins determine organotropic metastasis. Nature 2015;527:329–335.
[31] Patel D, Haque A, Gao Y, Revzin A. Using reconfigurable microfluidics to study the role of HGF in autocrine and paracrine signaling of hepatocytes. Integr Biol (Camb) 2015;7:815–824.
[32] Hyenne V, Ghoroghi S, Collot M, Bons J, Follain G, Harlepp S, et al. Studying the fate of tumor extracellular vesicles at high spatiotemporal resolution using the zebrafish embryo. Dev Cell 2019;48:554.
[33] Verweij FJ, Revenu C, Arras G, Dingli F, Loew D, Pegtel DM, et al. Live tracking of inter-organ communication by endogenous exosomes in vivo. Dev Cell 2019;48:573.
[34] Povero D, Eguchi A, Li H, Johnson CD, Papouchado BG, Wree A, et al. Circulating extracellular vesicles with specific proteome and liver microRNAs are potential biomarkers for liver injury in experimental fatty liver disease. PloS ONE 2014;9 e113651.
[35] Krishnan A, Abdullah TS, Mounajjed T, Hartono S, McConico A, White T, et al. A longitudinal study of whole body, tissue, and cellular physiology in a mouse model of fibrosing NASH with high fidelity to the human condition. Am J Physiol Gastrointest Liver Physiol 2017;312:G666–G680.